# Numerical integration over polygons by an 8-nodequadrilateral spline finite element



*Published version:*

DOI:10.1016/j.cam.2009.07.017

Chong-Jun Li, Paola Lamberti, Catterina Dagnino
*Numerical integration over polygons using an eight-node quadrilateral spline finite element*
J. Comput. Appl. Math., 233, no.2 (2009), 279-292, DOI 10.1016/j.cam.2009.07.017

# Numerical integration over polygons by an 8-node quadrilateral spline finite element[☆]


Chong-Jun Li[*,a], Paola Lamberti[b], Catterina Dagnino[b]

[a]*School of Mathematical Sciences, Dalian University of Technology, Dalian 116024, China*
[b]*Department of Mathematics, University of Torino, via C. Alberto, 10 Torino 10123, Italy*



## Abstract

In this paper, a cubature formula over polygons is proposed and analysed. It is based on an 8-node quadrilateral spline finite element ([5]) and exact for quadratic polynomials on arbitrary convex quadrangulations and for cubic polynomials on rectangular partitions. The convergence of sequences of the above cubatures is proved for continuous integrand functions and error bounds are derived. Some numerical examples are given, by comparisons with other known cubatures.



*Key words:* Numerical integration; Spline finite element method; Bivariate splines; Triangulated quadrangulation
*2000 MSC:* 65D05; 65D07; 65D30; 65D32


## 1. Introduction

The problem considered in this paper is the numerical evaluation of

$$I_\Omega(f) = \int_\Omega f(x, y)\mathrm{d}x\mathrm{d}y, \tag{1}$$


[☆]Work supported by the WWS - World Wide Style, funded by the Fondazione CRT of Torino (Italy) and by Science Foundation of Dalian University of Technology (No. SFDUT07001, China).



[*]Corresponding author.
*Email addresses:* chongjun@dlut.edu.cn (Chong-Jun Li), paola.lamberti@unito.it (Paola Lamberti), catterina.dagnino@unito.it (Catterina Dagnino)

where $f \in C(\Omega)$ and $\Omega$ is a polygonal domain in $\mathbb{R}^2$, i.e. a domain with the boundary composed of piecewise straight lines.

The evaluation of (1) can be obtained by subdividing the domain into many triangular or quadrilateral elements, then applying a local cubature on each element and summing up the integrals of all elements. If we consider quadrilateral elements, a local cubature can be constructed by tensor product of univariate quadratures, applied by transforming the standard rectangular element into the corresponding quadrilateral one ([11]).

Recently, in [7] a different approach based on Green's integral formula is used in the numerical evaluation of (1). A kind of Gauss-like cubature formulas over polygons is constructed by transforming a 2-dimensional into a 1-dimensional problem and by using univariate Gauss quadratures. Such cubatures, that we will denote by GR, can provide very accurate approximations for integrals of smooth functions. However, for not smooth functions, for example with singularities of the gradient inside the integration domain, they are not so accurate as for the smooth ones, as remarked in Section 4 of [7].

In this paper we propose a local cubature for (1), based on a special spline quadrilateral finite element and applied by a subdivision technique. Then we compare it with other known ones.

As we know, univariate Gauss quadratures possess the highest order of accuracy. For example, we can consider the tensor product $2 \times 2$ Gauss-Legendre cubature (denoted by G4 in this paper) on $[-1,1]^2$ ([2]), defined as follows:

$$\int_{-1}^{1}\int_{-1}^{1} f(x,y)\mathrm{d}x\mathrm{d}y \simeq \sum_{i,j=0,1} w_i w_j f(\xi_i, \xi_j),$$

where $w_0 = w_1 = 1$, $\xi_0 = -\sqrt{1/3}$, $\xi_1 = \sqrt{1/3}$. G4 is exact for all polynomials of coordinate degree three on a rectangular or parallelogram element. By using the bilinear transformation, G4 can be applied on arbitrary convex quadrilateral element with degree of accuracy two ([11]). The advantage of Gauss cubature is using only few nodes and having high accuracy. However, the nodes are fixed and located in the interior of the element domain (as shown in Fig. 1(a)), so that the integrand function value on each node is only used once for the element cubature. Therefore, since the total number of nodes for G4 is four times the number of elements, then the number of nodes will increase rapidly, if we apply a subdivision technique.

Another cubature, with degree of accuracy two, for quadrilateral elements can be the tensor product Simpson formula. It has nine nodes located on the element (hence we denote it by S9 in this paper), with eight nodes on the boundary and one node inside the element, as shown in Fig. 1(b). We remark the above rule coincides with the Gauss-Lobatto one with the same degree of accuracy [6].

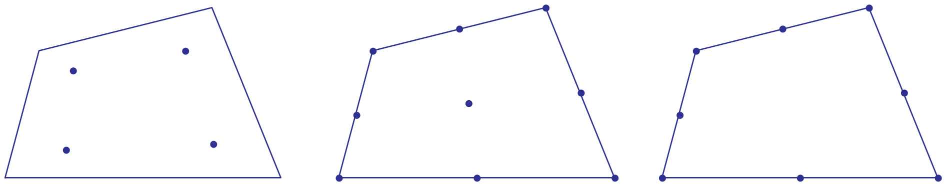

(a) G4 (b) S9 (c) L8

Figure 1: The location of nodes for G4, S9, L8-cubatures on quadrilateral element.

In finite element method, one basic and popular 8-node isoparametric element, denoted by Q8, is obtained by bilinear transformation from 8-node Serendipity element on rectangular element ([11]). Its nodes are located on the four vertices and the four midpoints of the edges of the quadrilateral element.

In [5], an 8-node quadrilateral quadratic spline element (denoted by L8) was presented, with 8 nodes on the boundary of the element, the same of Q8, as shown in Fig. 1(c).

Here, for any $f \in C(\Omega)$ we define and analyse an interpolating operator, based on L8-element and reproducing all polynomials of total degree at most two. Then, a cubature over polygons, based on L8, is constructed and studied. It is denoted by L8-cubature. Its degree of accuracy is three for rectangular or parallelogram elements and two for quadrilateral elements, so that such cubature is comparable with G4 and S9.

In Section 2, after reviewing some results on the 8-node quadrilateral spline finite element defined in [5], we propose a spline interpolating operator, based on it, and its error analysis. In Section 3, we present the cubature, defined by means of the above spline operator. Finally, in Section 4, some numerical examples are given, with comparisons among L8, G4, S9 and GR cubatures. The numerical results show that for the integrand test functions with low order of smoothness, L8-cubatures are usually comparable to the other ones. However the main advantage of L8-cubatures is the location of their nodes. Indeed such points are all inside the domain $\Omega$ for convex and not convex polygons, while, for either non convex or multiply connected domains, GR cubature nodes can fall outside the polygon, as mentioned in the Remark 2.4 of [7]. Therefore, the integrand function $f$ has to be computed also in the rectangular domain containing the polygon and the error estimate involves the best uniform polynomial approximation on such rectangular domain. Moreover, although L8 formula has four more nodes than G4 in a single element, however, the total number of L8 nodes on the polygon is less than those of G4 and S9, when the number of elements is large, because L8 nodes lie on the boundary of each element and they are shared by several ones. Therefore L8-cubatures can be easy applied in subvidision procedures and efficiently combined with other numerical algorithms, based on boundary nodes.

The analysis and construction of adaptive algorithms, based on L8-cubatures, is an interesting tool, that we will consider in a successive paper.

## 2. An interpolating operator defined by the 8-node quadrilateral spline finite element

Suppose that $\lozenge$ is a nondegenerate convex quadrangulation of a closed polygonal domain $\Omega$ in $\mathbb{R}^2$. Some algorithms for constructing quadrangulations associated with a given set of vertices have been discussed in [1].

Let $\Delta_Q$ be the triangulation of $\lozenge$ generated by adjoining both diagonals of each quadrangle, as shown in Fig. 2.

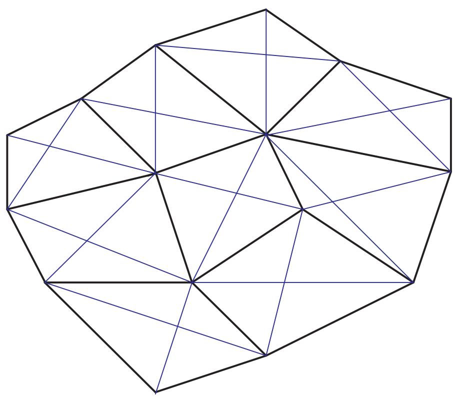

Figure 2: A triangulated quadrangulation.

We consider a bivariate quadratic spline space on $\Delta_Q$, denoted by $S_2^{0,1}(\Delta_Q)$, with different smoothness on different grid segments.

We define a spline $s \in S_2^{0,1}(\Delta_Q)$ as a piecewise polynomial of total degree two with the following two smoothness conditions:

*a*) $s$ is $C^0$ continuous on the quadrilateral grid segments;

*b*) $s$ is $C^1$ continuous on the diagonal grid segments of each quadrangle.

Since the splines in $S_2^{0,1}(\Delta_Q)$ are $C^0$ continuous on the quadrilateral grid segments, we only need to consider the piecewise representations on every quadrilateral element in $\Delta_Q$.

In order to define a spline basis for the whole quadrangulation, in the following we use a different notation from [5]. For every convex quadrangle $Q$, denote the four vertices and the four midpoints on each edge by $V_1, \ldots, V_4$ and $E_1, \ldots, E_4$, and denote the intersection of two diagonals $\overline{V_1V_3}$ and $\overline{V_2V_4}$ by $V_0 = (x_0, y_0)$, as shown in Fig. 3(a). Each quadrangle is divided into four subtriangles $\Delta_1, \ldots, \Delta_4$.

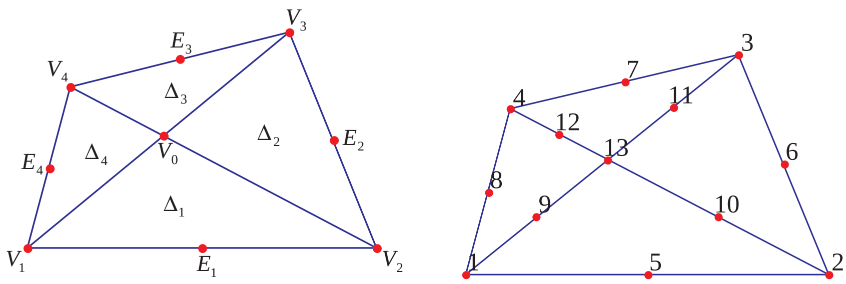


(a) (b)

Figure 3: A convex triangulated quadrangle and its domain points.

It is well known [3] that a polynomial $p$ of total degree two on a triangle $\Delta$ can be represented in the local Bernstein basis as

$$p(\lambda) = \sum_{|\alpha|=2} \gamma(\alpha) b_\alpha(\lambda)$$

where $b_\alpha(\lambda) = \frac{2}{\alpha!}\lambda^\alpha$, $\alpha = (\alpha_1, \alpha_2, \alpha_3)$, $\lambda = (\lambda_1, \lambda_2, \lambda_3)$ are the barycentric coordinates of $\Delta$, $\alpha! = \alpha_1!\alpha_2!\alpha_3!$ and $\lambda^\alpha = \lambda_1^{\alpha_1}\lambda_2^{\alpha_2}\lambda_3^{\alpha_3}$. The $\gamma(\alpha)$ are called *Bézier ordinates* of $p$. The piecewise linear interpolant to the points $(\alpha/2, \gamma(\alpha))$ is called *Bézier net* or *B-net* or *control net* of $p$. Such a B-net uniquely defines the patch, a fact which is made use of in the so called Bernstein-Bézier technique, where all information about the patch is extracted from this net.

Then, by the B-net method, there are thirteen domain points lying on the quadrangle, as their indexes show in Fig. 3(b). Let the Cartesian coordinates of the first eight points be

$$V_1 = (x_1, y_1),\ V_2 = (x_2, y_2),\ V_3 = (x_3, y_3),\ V_4 = (x_4, y_4),$$
$$E_1 = (V_1 + V_2)/2,\ E_2 = (V_2 + V_3)/2,\ E_3 = (V_3 + V_4)/2,\ E_4 = (V_4 + V_1)/2.$$

By the Smoothing Cofactor-Conformality method ([9, 10]), the dimension of the quadratic spline space, defined on the quadrangle $Q$ with $C^1$ smoothness on both diagonals $\overline{V_1V_3}$ and $\overline{V_2V_4}$, is eight. We can obtain eight linear independent splines, denoted by $B^Q_{V_1}, \ldots, B^Q_{V_4},\ B^Q_{E_1}, \ldots, B^Q_{E_4}$, corresponding to the eight nodes $V_1, \ldots, V_4,\ E_1, \ldots, E_4$, respectively. The eight spline basis can be represented in B-net form. The vectors of their Bézier coefficients, also denoted by $B^Q_{V_1}, \ldots, B^Q_{V_4},\ B^Q_{E_1}, \ldots, B^Q_{E_4}$ and corresponding to the thirteen domain points of each spline, are ([5])

$$(B^Q_{V_1}\ B^Q_{V_2}\ B^Q_{V_3}\ B^Q_{V_4}\ B^Q_{E_1}\ B^Q_{E_2}\ B^Q_{E_3}\ B^Q_{E_4})^T = \begin{pmatrix} I_4 & O & O \\ O & I_4 & C \end{pmatrix}, \tag{2}$$

with $I_4$ the identity matrix of order 4 and

$$C = \begin{pmatrix} a & b & 0 & 0 & ab \\ 0 & d & a & 0 & ad \\ 0 & 0 & c & d & cd \\ c & 0 & 0 & b & bc \end{pmatrix},$$

where $a, b, c, d$ are defined by the following ratios ([5]):

$$a = \frac{|\overline{V_4V_0}|}{|\overline{V_4V_2}|},\ b = \frac{|\overline{V_3V_0}|}{|\overline{V_3V_1}|},\ c = 1 - a,\ d = 1 - b. \tag{3}$$

They are shown in Fig. 4.

Since

$$cd + bc + ab + ad = 1,$$

the eight B-splines satisfy the unity partition property.

By the following invertible linear transformation

$$\begin{aligned} &L^Q_{V_1} = B^Q_{V_1} - \frac{1}{2}B^Q_{E_4} - \frac{1}{2}B^Q_{E_1}; \quad L^Q_{V_2} = B^Q_{V_2} - \frac{1}{2}B^Q_{E_1} - \frac{1}{2}B^Q_{E_2}; \\ &L^Q_{V_3} = B^Q_{V_3} - \frac{1}{2}B^Q_{E_2} - \frac{1}{2}B^Q_{E_3}; \quad L^Q_{V_4} = B^Q_{V_4} - \frac{1}{2}B^Q_{E_3} - \frac{1}{2}B^Q_{E_4}; \\ &L^Q_{E_1} = 2B^Q_{E_1};\ L^Q_{E_2} = 2B^Q_{E_2};\ L^Q_{E_3} = 2B^Q_{E_3};\ L^Q_{E_4} = 2B^Q_{E_4}, \end{aligned} \tag{4}$$

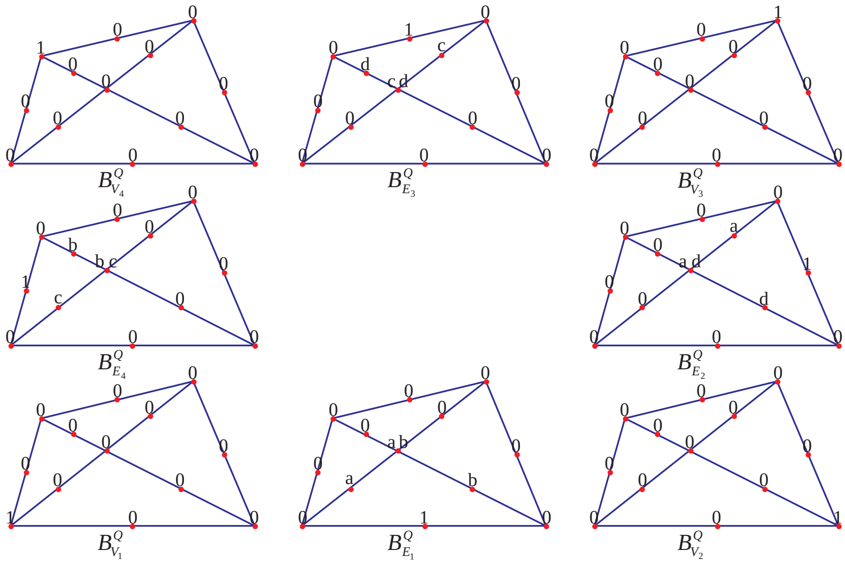


Figure 4: The supports of the eight spline basis $B_{V_1}^Q, \ldots, B_{V_4}^Q$, $B_{E_1}^Q, \ldots, B_{E_4}^Q$.

we obtain another set of basis functions (nodal basis), and the linear operator interpolating at all nodes $V_1, \ldots, V_4$, $E_1, \ldots, E_4$ as given in the following theorem ([5]).

**Theorem 1.** *Let $Q$ be the convex quadrilateral domain with vertices $V_1, V_2, V_3$, $V_4$ and*

$$L_Q : C(Q) \to S_2^{0,1}(\Delta_Q)$$

*be defined by*

$$L_Q(f) := \sum_{i=1}^{4} f(V_i) L_{V_i}^Q + \sum_{j=1}^{4} f(E_j) L_{E_j}^Q. \tag{5}$$

*Then*

$$L_Q(f)(V_i) = f(V_i),\ L_Q(f)(E_j) = f(E_j),\ i, j = 1, \ldots, 4, \tag{6}$$

*and*

$$L_Q(f) = f,\ \forall f \in \mathbb{P}_2, \tag{7}$$

*where $\mathbb{P}_2$ is the space of polynomials of total degree at most two.*

Now we come to the locally supported spline basis functions of the whole quadrangulation. If we denote by $N$, $V$ and $E$ the numbers of quadrilateral elements, vertices and edges of the quadrangulation $\diamondsuit = \bigcup_{k=1}^{N} Q_k$, then $\dim S_2^{0,1}(\Delta_Q) = V + E$ ([5]). For each element $Q_k$, there are two sets of local splines $\{B_{V_i}^{Q_k}\} \cup \{B_{E_j}^{Q_k}\}$ and $\{L_{V_i}^{Q_k}\} \cup \{L_{E_j}^{Q_k}\}$, defined by (2) and (4), respectively.

Since the splines in $S_2^{0,1}(\Delta_Q)$ are $C^0$ continuous on the quadrilateral grid segments, every spline basis function has the same Bézier coefficients on the intersection grid segments between two adjacent quadrilateral elements. So two locally supported spline bases of the space $S_2^{0,1}(\Delta_Q)$ can be obtained by merging the corresponding local splines, as follows. For each vertex $V_i$ of $\diamondsuit$, denote by $N_i$ the number of the quadrilateral elements $Q_{k_1}, \ldots, Q_{k_{N_i}}$, sharing such a vertex. Then the locally supported spline corresponding to $V_i$ on the whole domain is defined by

$$B_{V_i}(x,y) = \begin{cases} B_{V_i}^{Q_{k_1}}(x,y), & (x,y) \in Q_{k_1}, \\ \vdots & \\ B_{V_i}^{Q_{k_{N_i}}}(x,y), & (x,y) \in Q_{k_{N_i}}, \\ 0, & \text{otherwise} \end{cases} \tag{8}$$

and

$$L_{V_i}(x,y) = \begin{cases} L_{V_i}^{Q_{k_1}}(x,y), & (x,y) \in Q_{k_1}, \\ \vdots & \\ L_{V_i}^{Q_{k_{N_i}}}(x,y), & (x,y) \in Q_{k_{N_i}}, \\ 0, & \text{otherwise.} \end{cases} \tag{9}$$

The locally supported spline $B_{E_j}$ and $L_{E_j}$corresponding to $E_j$ can be defined similarly. Then the two bases on the whole quadrangulation are $\{B_{V_i}\}_{i=1}^{V} \cup \{B_{E_j}\}_{j=1}^{E}$ and $\{L_{V_i}\}_{i=1}^{V} \cup \{L_{E_j}\}_{j=1}^{E}$.

For example, in a uniform rectangular partition, for any vertex $V_i$ and midpoint $E_j$ of any edge, the Bézier coefficients of the locally supported B-splines $B_{V_i}$ and $B_{E_j}$ are shown in Fig. 5(a) and 5(b), according to local splines in (2) for each rectangular element. Since the Bézier coefficients vanish on the outer eight sub-triangles of $B_{V_i}$, the support of $B_{V_i}$ should exclude those triangles in dotted lines in Fig. 5(a).

In general, we denote by $Star(V_i)$ the support of $B_{V_i}$, i.e. the star domain composed of all quadrangles which share the vertex $V_i$, as shown in Fig. 6(a).

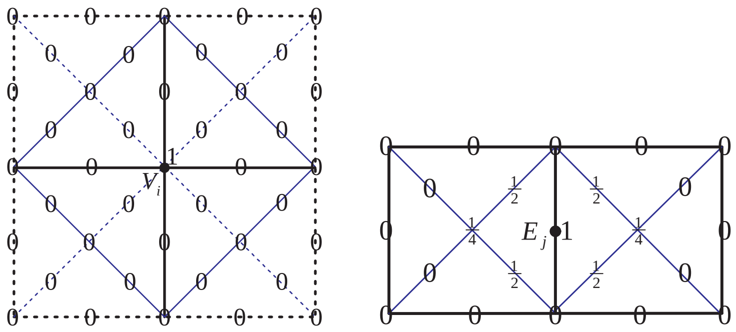


(a) $B_{V_i}$ (b) $B_{E_j}$

Figure 5: The Bézier coefficients and supports of B-splines on a uniform rectangular partition.

In fact, the support of $B_{V_i}$ is the smaller one by excluding the dotted triangles from $Star(V_i)$. Moreover we denote by $Star(E_j)$ the support of $B_{E_j}$, i.e. the union of two adjacent quadrangles which share the edge $E_j$, as shown in Fig. 6(b). We use for the edge the same notation as for its midpoint. Finally, we define 'radius' of $Star(V_i)$ (respectively $Star(E_j)$) the radius of the minimum circle containing $Star(V_i)$ (respectively $Star(E_j)$) and centered at $V_i$ (respectively $E_j$).

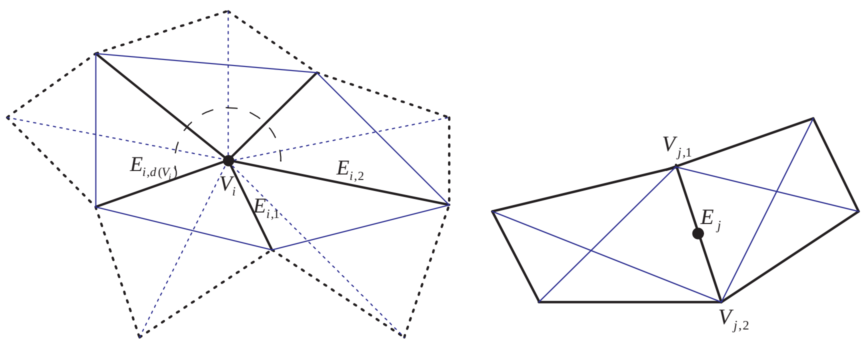


(a) $Star(V_i)$ (b) $Star(E_j)$

Figure 6: The two kinds of B-spline supports.

If we denote by $d(V_i)$ $(= N_i)$ the number of quadrilateral edges containing the vertex $V_i$, then the interior edges in $Star(V_i)$ are $E_{i,1}, E_{i,2}, \ldots, E_{i,d(V_i)}$. Moreover denote the two vertices of the edge $E_j$ by $V_{j,1}$ and $V_{j,2}$. Then we get the following relations between the two locally supported basis:

$$\begin{cases} L_{V_i} = B_{V_i} - \frac{1}{2}\sum_{j=1}^{d(V_i)} B_{E_{i,j}}, \; i = 1, 2, \ldots, V; \\ L_{E_j} = 2B_{E_j}, \; j = 1, 2, \ldots, E. \end{cases} \tag{10}$$

Hence, the supports of $L_{V_i}$ and $L_{E_j}$ are $Star(V_i)$ and $Star(E_j)$, respectively.

Now we can define the interpolating operator $L$ on the whole polygonal domain $\Omega$ by

$$L(f)(x,y) := \sum_{i=1}^{V} f(V_i)L_{V_i}(x,y) + \sum_{j=1}^{E} f(E_j)L_{E_j}(x,y), \; (x,y) \in \Omega. \tag{11}$$

By Theorem 1, since for any element $Q$ of the quadrangulation $L|_Q = L_Q$, the interpolation operator $L$ reproduces $\mathbb{P}_2$ on $\Omega$, as well. In particular, all nodal splines satisfy the partition of unity property:

$$\sum_{i=1}^{V} L_{V_i}(x,y) + \sum_{j=1}^{E} L_{E_j}(x,y) \equiv 1, \; (x,y) \in \Omega. \tag{12}$$

From (10), (11), and $\sum_{i=1}^{V} f(V_i) \sum_{j=1}^{d(V_i)} B_{E_j} = \sum_{j=1}^{E}(f(V_{j,1})+f(V_{j,2}))B_{E_j}$, we get

$$\begin{aligned} L(f) &= \sum_{i=1}^{V} f(V_i)(B_{V_i} - \tfrac{1}{2}\sum_{j=1}^{d(V_i)} B_{E_j}) + \sum_{j=1}^{E} f(E_j)2B_{E_j} \\ &= \sum_{i=1}^{V} f(V_i)B_{V_i} + \sum_{j=1}^{E}(2f(E_j) - \tfrac{1}{2}f(V_{j,1}) - \tfrac{1}{2}f(V_{j,2}))B_{E_j}. \end{aligned} \tag{13}$$

Therefore we can define the linear operator $B$ by

$$B(f) := \sum_{i=1}^{V} f(V_i)B_{V_i} + \sum_{j=1}^{E}(2f(E_j) - \frac{1}{2}f(V_{j,1}) - \frac{1}{2}f(V_{j,2}))B_{E_j}, \; (x,y) \in \Omega. \tag{14}$$

By Theorem 1, since $B = L$, we have that for all $f \in \mathbb{P}_2$,

$$B(f)(x,y) = f(x,y), \; (x,y) \in \Omega. \tag{15}$$

From (14), the $B_{V_i}$, $B_{E_i}$ also have the partition of unity property,

$$\sum_{i=1}^{V} B_{V_i}(x,y) + \sum_{j=1}^{E} B_{E_j}(x,y) \equiv 1, \; (x,y) \in \Omega. \tag{16}$$

Note that all $B_{V_i}$'s and $B_{E_j}$'s are positive in the interior of their support. By (14) and (16), it is easy to prove that $\|B\|_\infty \le 3$.

Now we consider the uniform approximation to $S_2^{0,1}(\Delta_Q)$ by the spline defined by the operator $L$ (or $B$). The Euclidean norm of the ordered pair $(x, y)$ is defined by

$$|(x,y)| = (x^2 + y^2)^{1/2}.$$

Let $K \subset \mathbb{R}^2$ be a compact set. Denote the modulus of continuity of $f \in C(K)$ by

$$\omega_K(f;\varepsilon) = \sup\{|f(x,y) - f(u,v)| : (x,y),(u,v) \in K, |(x,y) - (u,v)| < \varepsilon\}.$$

Let $k$ be a positive integer, and denote

$$f_{x^{k-l}y^l} = \frac{\partial^k f}{\partial x^{k-l}\partial y^l}, \quad l = 0, \ldots, k,$$

$$\left(p\frac{\partial}{\partial x} + q\frac{\partial}{\partial y}\right)^k f = \sum_{l=0}^{k} \binom{k}{l} p^{k-l} q^l f_{x^{k-l}y^l},$$

$$\omega_{k,\Omega}(f,\delta) = \max_{l=0,\ldots,k} \omega_\Omega(f_{x^{k-l}y^l};\delta),$$

$$\|D^k f\| = \max_{l=0,\ldots,k} \sup_{(x,y)\in\Omega} |f_{x^{k-l}y^l}(x,y)|.$$

We have the following results.

**Theorem 2.** *Let $f \in C(\Omega)$ and $\|\cdot\|_\Omega$ be the maximum norm on $\Omega$. Denote $\delta$ by the length of the longest diagonal or edge in the quadrangulation $\diamondsuit$ of $\Omega$. Then*

$$\|f - B(f)\|_\Omega \le 2\omega_\Omega(f,\delta). \tag{17}$$

*If, in addition:*

*i)* $f \in C^1(\Omega)$, *then*

$$\|f - B(f)\|_\Omega \le 8\delta\omega_{1,\Omega}(f,\delta); \tag{18}$$

*ii)* $f \in C^2(\Omega)$, *then*

$$\|f - B(f)\|_\Omega \le 8\delta^2\omega_{2,\Omega}(f,\delta); \tag{19}$$

*iii)* $f \in C^3(\Omega)$, *then*

$$\|f - B(f)\|_\Omega \leq \frac{16}{3}\delta^3 \|D^3 f\|. \tag{20}$$

**Proof**. Note that all $B_{V_i}$'s and $B_{E_j}$'s are nonnegative and satisfy the partition of unity property (16). Since $\delta$ is bigger than the radius of either $Star(V_i)$ or $Star(E_j)$, then

$$\begin{aligned}
& \|f - B(f)\|_\Omega \\
= \;& \|\sum_{i=1}^{V}(f(x,y) - f(V_i))B_{V_i} + \sum_{j=1}^{E}(f(x,y) - 2f(E_j) + \frac{1}{2}f(V_{j,1}) + \frac{1}{2}f(V_{j,2}))B_{E_j}\|_\Omega \\
\leq \;& \omega_\Omega(f,\delta)\sum_{i=1}^{V} B_{V_i} + 2\omega_\Omega(f,\delta)\sum_{j=1}^{E} B_{E_j} \\
\leq \;& 2\omega_\Omega(f,\delta)(\sum_{i=1}^{V} B_{V_i} + \sum_{j=1}^{E} B_{E_j}) = 2\omega_\Omega(f,\delta).
\end{aligned}$$

*i)* When $f \in C^1(\Omega)$, let $Q$ denote the quadrilateral element in $\Delta_Q$, such that

$$\|f - B(f)\|_\Omega = \|f - B(f)\|_Q.$$

Let $(x_0, y_0)$ be a vertex or a midpoint of an edge of $Q$. Then

$$\forall (x,y) \in Q,\; |x - x_0|,\; |y - y_0|,\; |(x,y) - (x_0,y_0)| \leq \delta.$$

Denote

$$p_1(x,y) = f(x_0,y_0) + f_x(x_0,y_0)(x - x_0) + f_y(x_0,y_0)(y - y_0).$$

Then, by the Taylor expansion, we get:

$$f(x,y) = p_1(x,y) + (f_x(u,v) - f_x(x_0,y_0))(x - x_0) + (f_y(u,v) - f_y(x_0,y_0))(y - y_0),$$

for a certain $(u,v)$, where

$$(u,v) = t(x,y) + (1-t)(x_0,y_0),\; t \in (0,1). \tag{21}$$

By (15), $\|B\| \leq 3$ and (21), we have

$$\begin{aligned}
\|f - B(f)\|_Q &\leq \|f - p_1\|_Q + \|B(f - p_1)\|_Q \\
&\leq 4\|f - p_1\|_Q \\
&\leq 4(\delta\omega_\Omega(f_x;\delta) + \delta\omega_\Omega(f_y;\delta)) \\
&\leq 8\delta\omega_{1,\Omega}(f,\delta).
\end{aligned}$$

*ii*) When $f \in C^2(\Omega)$, by the Taylor expansion

$$\begin{aligned} f(x,y) &= p_2(x,y) + \frac{1}{2}\{(f_{xx}(u,v) - f_{xx}(x_0,y_0))(x-x_0)^2 \\ &+ 2(f_{xy}(u,v) - f_{xy}(x_0,y_0))(x-x_0)(y-y_0) \\ &+ (f_{yy}(u,v) - f_{yy}(x_0,y_0))(y-y_0)^2\}, \end{aligned}$$

where $(u,v)$ is defined as in (21) and

$$\begin{aligned} p_2(x,y) &= p_1(x,y) + \frac{1}{2}\{f_{xx}(x_0,y_0)(x-x_0)^2 \\ &+ 2f_{xy}(x_0,y_0)(x-x_0)(y-y_0) + f_{yy}(x_0,y_0)(y-y_0)^2\}. \end{aligned}$$

By (15), $\|B\| \le 3$ and (21), we have

$$\|f - B(f)\|_Q \le 4\|f - p_2\|_Q \le 4 \cdot \frac{1}{2} \cdot 4\omega_{2,\Omega}(f,\delta) \cdot \delta^2 = 8\delta^2\omega_{2,\Omega}(f,\delta).$$

*iii*) When $f \in C^3(\Omega)$, by the Taylor expansion

$$f(x,y) = p_2(x,y) + \frac{1}{6}((x-x_0)\frac{\partial}{\partial x} + (y-y_0)\frac{\partial}{\partial y})^3 f(u,v),$$

then

$$\|f - B(f)\|_Q \le 4\|f - p_2\|_Q \le 4 \cdot \frac{1}{6} \cdot 8\delta^3\|D^3 f\| = \frac{16}{3}\delta^3\|D^3 f\|.$$

□

For the convergence, we consider a subdivision of each element by equally dividing the edges into $m$ or $n$ sub-edges so that each element is equally subdivided into $m \times n$ subelements. From Theorem 2 and the property of the modulus of continuity, we immediately get the following corollary.

**Corollary 1.** *Denote $\delta$ by the length of the longest diagonal or edge in the quadrangulation $\diamondsuit$ of $\Omega$. If we equally subdivide each element of $\diamondsuit$ into $m \times n$ subelements, with $m, n \in \mathbb{N}$, and we consider $B(f)$ on the new quadrangulation, then $\delta \to 0$ as $m, n \to \infty$ and*

$$\lim_{\delta \to 0} \|f - B(f)\|_\Omega = 0, \quad \forall f \in C(\Omega).$$

*Moreover, if $f \in C(\Omega)$, then $\|f - B(f)\|_\Omega = o(1)$ and, if $f \in C^j(\Omega)$, $1 \le j \le 2$, then $\|f - B(f)\|_\Omega = o(\delta^j)$.*

## 3. The numerical cubature

By using the interpolation operator $L$ defined in (11), we can define cubature formulas for integrals (1) as follows:

$$I_\Omega(f) \approx \tilde{I}_\Omega(f) := \int\int_\Omega L(f)(x,y)\mathrm{d}x\mathrm{d}y = \sum_{i=1}^{V} C_{V_i} f(V_i) + \sum_{j=1}^{E} C_{E_j} f(E_j), \quad (22)$$

where

$$C_{V_i} = \int\int_\Omega L_{V_i}(x,y)\mathrm{d}x\mathrm{d}y, \;\; i = 1,2,\dots,V,$$

$$C_{E_j} = \int\int_\Omega L_{E_j}(x,y)\mathrm{d}x\mathrm{d}y, \;\; j = 1,2,\dots,E.$$

By (15), the degree of accuracy of the cubature is at least two, i.e.

$$I_\Omega(f) = \tilde{I}_\Omega(f), \;\; \forall f \in \mathbb{P}_2. \quad (23)$$

Moreover, from Corollary 1, since $B = L$, then the cubature sequence, obtained by the subdivision technique there introduced, converges to the exact value of the integral, i.e.

$$\lim_{\delta\to 0} \tilde{I}_\Omega(f) = I_\Omega(f) \quad (24)$$

and error bounds can be immediately derived from the results of Theorem 2.

In practice we compute the cubature formula as follows:

$$\tilde{I}_\Omega(f) = \sum_{k=1}^{N} \tilde{I}_{Q_k}(f) := \sum_{k=1}^{N} \int\int_{Q_k} L_{Q_k}(f)(x,y)\mathrm{d}x\mathrm{d}y,$$

where $L_{Q_k}$ is the interpolating operator restricted on $Q_k$, as defined by (5).

Let $Q$ be an arbitrary convex quadrilateral element with vertices $V_1, V_2, V_3, V_4$, as shown in Fig. 3(a) and $V_0$ be the intersection point of the two diagonals. Then the areas of the four subtriangles $\Delta_1, \dots, \Delta_4$ are

$$S_1 = \frac{1}{2}\begin{vmatrix} 1 & x_0 & y_0 \\ 1 & x_1 & y_1 \\ 1 & x_2 & y_2 \end{vmatrix}, S_2 = \frac{1}{2}\begin{vmatrix} 1 & x_0 & y_0 \\ 1 & x_2 & y_2 \\ 1 & x_3 & y_3 \end{vmatrix}, \; S_3 = \frac{1}{2}\begin{vmatrix} 1 & x_0 & y_0 \\ 1 & x_3 & y_3 \\ 1 & x_4 & y_4 \end{vmatrix}, \; S_4 = \frac{1}{2}\begin{vmatrix} 1 & x_0 & y_0 \\ 1 & x_4 & y_4 \\ 1 & x_1 & y_1 \end{vmatrix}.$$

Denote by $E_1, \dots, E_4$ the four midpoints of the edges of $Q$ (Fig. 3(b)). By (5), the cubature formula on $Q$ is

$$\tilde{I}_Q(f) = \int\int_Q L_Q(x,y)\mathrm{d}x\mathrm{d}y = \sum_{i=1}^{4} C_{V_i}^Q f(V_i) + \sum_{j=1}^{4} C_{E_j}^Q f(E_j), \tag{25}$$

with coefficients $C_{V_i}^Q = \int\int_Q L_{V_i}^Q(x,y)\mathrm{d}x\mathrm{d}y$ and $C_{E_j}^Q = \int\int_Q L_{E_j}^Q(x,y)\mathrm{d}x\mathrm{d}y$.

By the B-net method, the integral of a bivariate polynomial of total degree $p$ over a triangle equals the sum of its Bézier coefficients multiplied by $\frac{2}{(p+1)(p+2)}$ times the area of the triangle. Therefore, by (2) and (4), we obtain the eight cubature coefficients

$$\begin{aligned}
C_{V_1}^Q &= -\frac{1}{6}b(S_1+S_2+S_3+S_4),\ C_{V_2}^Q = -\frac{1}{6}a(S_1+S_2+S_3+S_4),\\
C_{V_3}^Q &= -\frac{1}{6}d(S_1+S_2+S_3+S_4),\ C_{V_4}^Q = -\frac{1}{6}c(S_1+S_2+S_3+S_4),\\
C_{E_1}^Q &= \frac{1}{3}((1+a+b+ab)S_1+(b+ab)S_2+abS_3+(a+ab)S_4),\\
C_{E_2}^Q &= \frac{1}{3}((d+ad)S_1+(1+a+d+ad)S_2+(a+ad)S_3+adS_4),\\
C_{E_3}^Q &= \frac{1}{3}(cdS_1+(c+cd)S_2+(1+c+d+cd)S_3+(d+cd)S_4),\\
C_{E_4}^Q &= \frac{1}{3}((c+bc)S_1+bcS_2+(b+bc)S_3+(1+b+c+bc)S_4),
\end{aligned} \tag{26}$$

where $a, b, c, d$ are defined in (3).

It is clear that the formula (25) and its coefficients (26) only depend on the four vertices $V_1, V_2, V_3$ and $V_4$.

In particular, if $Q$ is a rectangle or a parallelogram with area $S_Q$, then

$$a = b = c = d = \frac{1}{2},\ S_1 = S_2 = S_3 = S_4 = \frac{1}{4}S_Q,$$

and

$$C_{V_1}^Q = C_{V_2}^Q = C_{V_3}^Q = C_{V_4}^Q = -\frac{1}{12}S_Q,\ C_{E_1}^Q = C_{E_2}^Q = C_{E_3}^Q = C_{E_4}^Q = \frac{1}{3}S_Q.$$

In this case it is easy to verify that

$$\forall f \in \mathbb{P}_3,\ I(f) = \tilde{I}_Q(f), \tag{27}$$

i.e. the degree of accuracy of cubature (25) on $Q$ is three.

Furthermore, by (26), for an arbitrary convex quadrilateral element $Q$, we have

$$\sum_{i=1}^{4} |C_{V_i}^{Q}| + \sum_{j=1}^{4} |C_{E_j}^{Q}| = \frac{5}{3} S_Q. \tag{28}$$

Therefore, for the whole polygonal domain $\Omega$, the sum of all cubature coefficients are bounded as follows

$$\sum_{i=1}^{V} |C_{V_i}| + \sum_{j=1}^{E} |C_{E_j}| = \frac{5}{3}\mathrm{meas}(\Omega), \tag{29}$$

where meas($\Omega$) denotes the area of $\Omega$. From the multivariate version of Polya-Steklov theorem, the cubature over $\Omega$ is stable ([4, 8]).

## 4. Numerical examples

In this section, some numerical examples are presented to test L8-cubature, compared with G4, S9 and GR cubatures, for increasing values of the node number.

The integration domains are the same as the ones considered in [7]: Figure 7(a) shows the convex domain $\Omega_c$, with two initial quadrilateral elements, whose coordinates of the six vertices are $(0, 0.25), (0.1, 0), (0.7, 0.2)$, $(1, 0.5)$, $(0.75, 0.85)$, $(0.5, 1)$ and Figure 7(b) shows the non-convex domain $\Omega_{nc}$, with five initial quadrilateral elements, whose coordinates of the eleven vertices are $(0, 0.75)$, $(0.25, 0.5)$, $(0.25, 0)$, $(0.75, 0.5)$, $(0.75, 0)$, $(1, 0.5)$, $(0.75, 0.75)$, $(0.75, 0.85)$, $(0.5, 1)$, $(7/8, 5/8)$, $(1/2, 5/8)$.

As test functions we consider

$$\begin{aligned}
f_1(x,y) &= e^{-100((x-0.5)^2+(y-0.5)^2)},\\
f_2(x,y) &= \sqrt{(x-0.5)^2+(y-0.5)^2},\\
f_3(x,y) &= |x^2+y^2-1/4|,\\
f_4(x,y) &= \sqrt{|3-4x-3y|},\\
f_5(x,y) &= e^{-\frac{(5-10x)^2}{2}} + 0.75e^{-\frac{(5-10y)^2}{2}} + 0.75e^{-\frac{(5-10x)^2}{2}-\frac{(5-10y)^2}{2}}\\
&\quad +(x+y)^3(x-0.6)_+,\\
f_6(x,y) &= ((1/9)\sqrt{64-81((x-1/2)^2+(y-1/2)^2)}-1/2)(x+y-1)_+,
\end{aligned}$$

where $f_+ = \max(f, 0)$.

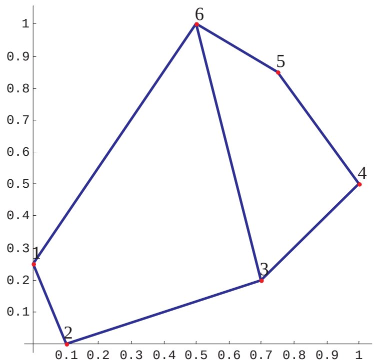


(a)

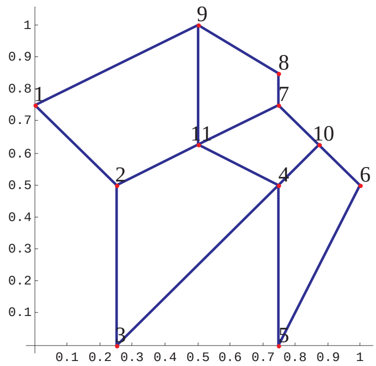


(b)

Figure 7: $(a)$ The convex domain $\Omega_c$ and $(b)$ the non-convex domain $\Omega_{nc}$ with initial quadrilateral elements.

In order to test our method and compare it with other known ones, we use both smooth and not so smooth test functions. Some of them were used in the reference [7].

We use the subdivision technique introduced in Section 2, based on G4, L8, S9 cubatures, i.e. each initial quadrilateral element is equally subdivided into $m \times n$ subelements. We note that in such an element the number of function evaluations, i.e. the number of nodes, is

i) $4mn$ for G4,

ii) $4mn + 2m + 2n + 1$ for S9,

iii) $3mn + 2m + 2n + 1$ for L8.

Therefore for large $m$ and $n$, L8 formula has less nodes than G4 and S9. Each function is also integrated by GR-cubature.

The reference integral values of test functions could be computed by the Matlab **dblquad** procedure (adaptive cubature routine) applied to the integrand, multiplied by the characteristic function of the domain (which can be implemented via the Matlab **inpolygon** function, cf. [13]), as in [7]. However, since the above procedure, applied directly to the whole enclosing square, can give unreliable results, as remarked in [7], then here the reference integral values are computed both by Mathematica **NIntegrate** function with 20-digit WorkingPrecision [14] and by Maple **int** function (twice) with 50-digit [12], based on subdividing the polygonal domain into several trapezoidal sub-domains by vertical lines. Successively, by comparison, we choose the reference values by the results containing the most same digits with others, as shown in Table 1, where we report the absolute errors between the reference integral values obtained by Mathematica and Maple.

Table 1: Reference integral values of the test functions, computed by Mathematica, and errors compared with the ones obtained by Maple.

| $f$ | reference values over $\Omega_c$ | Error | reference values over $\Omega_{nc}$ | Error |
|---|---|---|---|---|
| $f_1$ | 0.0314145286323930608872 | 2.7(-16) | 0.031220838971546493 | 7.2(-15) |
| $f_2$ | 0.156825125586275891714 | 1.8(-13) | 0.13938145677146538 | 1.4(-14) |
| $f_3$ | 0.199062549435189053162 | 5.2(-16) | 0.20842559601611674 | 2.2(-16) |
| $f_4$ | 0.545386805005417548157 | 1.8(-15) | 0.4545305519051566 | 2.5(-15) |
| $f_5$ | 0.449279503261762497773 | 3.1(-15) | 0.4115120322110313 | 2.5(-15) |
| $f_6$ | 0.0158750489593231157424 | 5.3(-16) | 0.024308669040669872 | 4.3(-16) |

L8-cubature relative errors for the integral values over $\Omega_c$ and $\Omega_{nc}$ are shown in Tables 2 and 3, respectively, for increasing values of the node number. They are obtained by a procedure we implemented in Matlab. We subdivide each initial quadrilateral element into $n \times n$ subelements, i.e. we assume $m = n$. Then the total number of nodes for L8-cubature is

$$PTS = N \cdot (3n^2 + 4n + 1) - intE \cdot (2n + 1) + intV,$$

where $N$ is the number of initial quadrilateral elements, $intE$ and $intV$ are the numbers of their interior edges and vertices, respectively. For example, we have $N = 2,\ intE = 1,\ intV = 0$ for $\Omega_c$ and $N = 5,\ intE = 5,\ intV = 1$ for $\Omega_{nc}$.

In Figure 8 we present Matlab plots of meshes and nodes by L8-cubature for the non-convex domain $\Omega_{nc}$, where (a) $n = 4$ and (b) $n = 16$.

In order to compare L8-cubature with the other ones, i.e. G4, S9 and GR, in figures 9 and 10 we show relative error graph comparisons for the six test integrals over $\Omega_c$ and on $\Omega_{nc}$, respectively. The $x$-axis denotes the number of function values (or cubature nodes), labeled by $PTS$. The line with '$\times$' denotes the relative error by G4, the line with '+' by L8, the line with '$*$' by S9, and the line with '$\cdot$' by GR.

We note that GR cubature is better than G4, L8 and S9 for the smooth integrand function $f_1$. In case of non smooth functions the results obtained

Table 2: L8-cubature relative errors for the considered test functions on the convex domain $\Omega_c$.

| $n$ | 1 | 2 | 4 | 8 | 16 | 32 |
|---|---|---|---|---|---|---|
| $PTS$ | 13 | 37 | 121 | 433 | 1633 | 6337 |
| $f_1$ | 2.30(-1) | 9.95(-1) | 7.25(-3) | 3.02(-5) | 3.34(-7) | 4.23(-9) |
| $f_2$ | 2.53(-3) | 1.12(-2) | 9.01(-4) | 2.29(-4) | 8.83(-6) | 7.57(-6) |
| $f_3$ | 9.38(-3) | 6.44(-3) | 1.65(-5) | 2.12(-5) | 2.57(-5) | 1.09(-6) |
| $f_4$ | 7.17(-4) | 2.38(-2) | 3.93(-3) | 1.86(-4) | 1.05(-4) | 4.18(-5) |
| $f_5$ | 6.68(-2) | 9.29(-2) | 8.93(-4) | 7.18(-6) | 2.21(-6) | 1.29(-6) |
| $f_6$ | 7.98(-2) | 2.26(-3) | 5.31(-5) | 5.35(-4) | 7.22(-5) | 3.81(-5) |

Table 3: L8-cubature relative errors for the considered test functions on the non-convex domain $\Omega_{nc}$.

| $n$ | 1 | 2 | 4 | 8 | 16 | 32 |
|---|---|---|---|---|---|---|
| $PTS$ | 26 | 81 | 281 | 1041 | 4001 | 15681 |
| $f_1$ | 5.12(-1) | 1.04(-1) | 1.41(-3) | 1.38(-5) | 7.32(-7) | 4.37(-8) |
| $f_2$ | 2.35(-2) | 1.31(-3) | 1.54(-6) | 1.27(-5) | 2.67(-6) | 7.88(-7) |
| $f_3$ | 1.29(-2) | 1.19(-3) | 1.28(-3) | 1.97(-4) | 3.71(-6) | 1.38(-6) |
| $f_4$ | 2.42(-3) | 1.16(-3) | 3.79(-3) | 6.53(-4) | 1.28(-4) | 4.78(-5) |
| $f_5$ | 9.11(-2) | 8.08(-3) | 3.44(-4) | 1.05(-5) | 9.99(-6) | 8.77(-7) |
| $f_6$ | 1.75(-2) | 6.18(-3) | 6.68(-4) | 2.27(-4) | 2.17(-5) | 3.11(-6) |

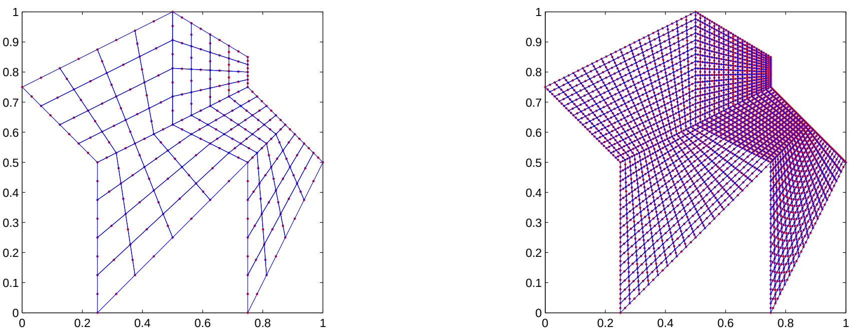


(a) (b)

Figure 8: The meshes and nodes by L8 cubature for the non-convex domain $\Omega_{nc}$ when (a) $n = 4$ and (b) $n = 16$.

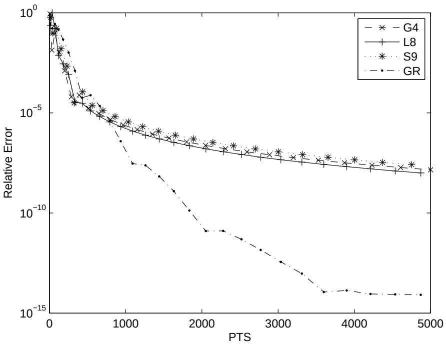


(a) $f_1$

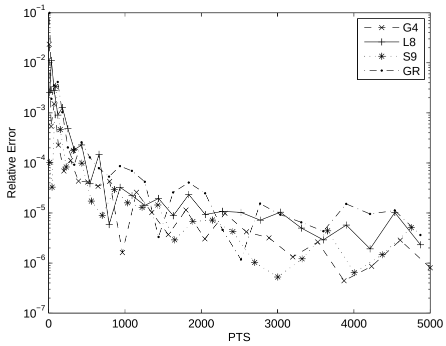


(b) $f_2$

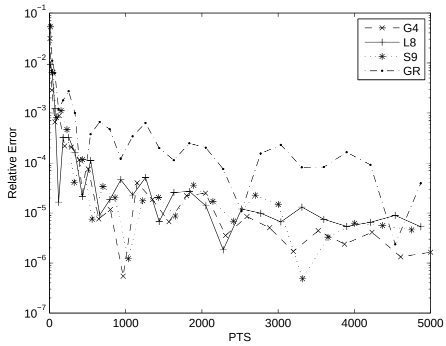


(c) $f_3$

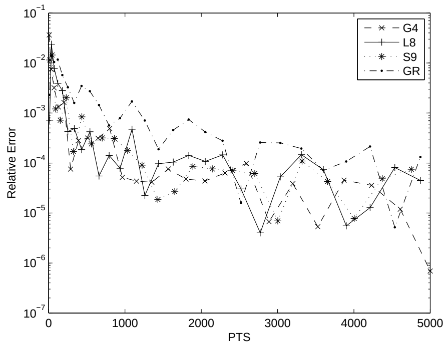


(d) $f_4$

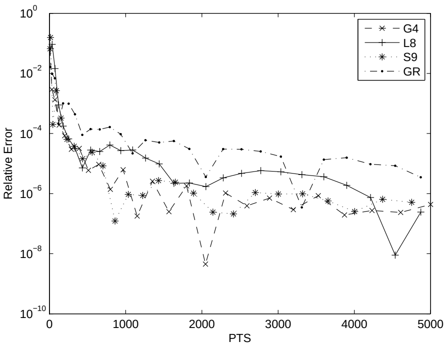


(e) $f_5$

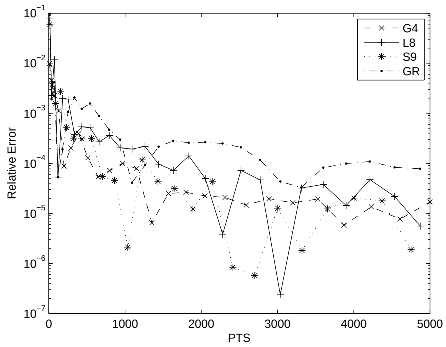


(f) $f_6$

Figure 9: G4, L8, S9, GR-cubature relative errors for integrals over the convex domain $\Omega_c$.

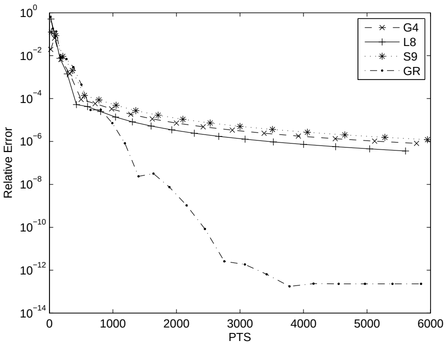


(a) $f_1$

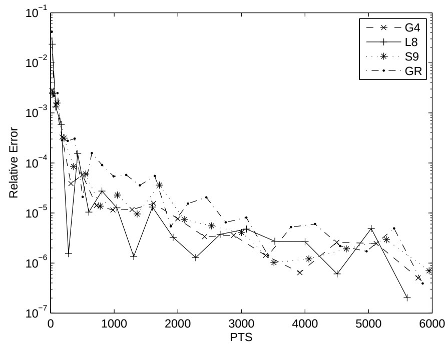


(b) $f_2$

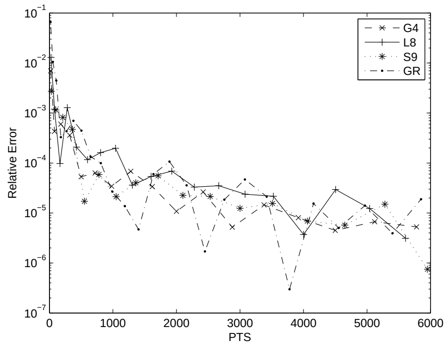


(c) $f_3$

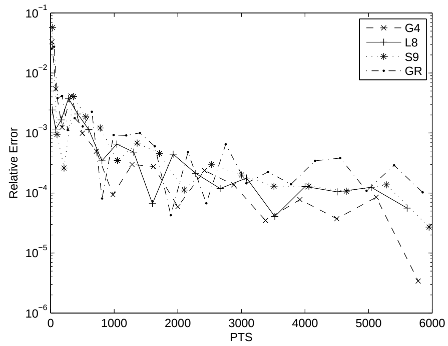


(d) $f_4$

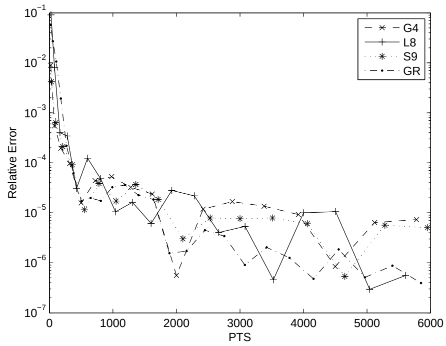


(e) $f_5$

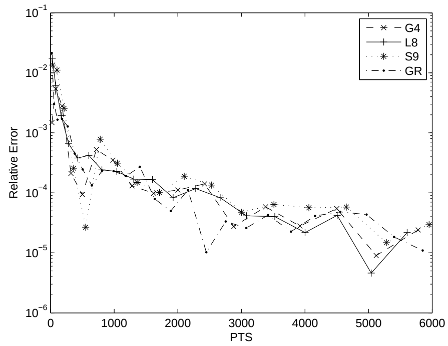


(f) $f_6$

Figure 10: G4, L8, S9, GR-cubature relative errors for integrals over the not convex domain $\Omega_{nc}$.

by all methods seem to be comparable. However we can remark that a significant difference of all such cubatures is the node location. For G4 and GR, based on Gauss quadratures, the node location is fixed and in general some of GR nodes could fall outside $\Omega$, when $\Omega$ is not convex or with holes. Moreover all nodes change when the elements in the subdivision for G4 and the accuracy degree for GR increase. In such a comparison the advantage of L8 and S9 cubatures, with respect to the other ones, is that at any step the previous nodes are kept in the procedure of subdivision, since they are the vertices of the finer quadrilateral subdivision, which the new nodes belong to. Further, L8 is more suitable than S9 in case the nodes have to be located only on the boundary of the quadrilateral elements, e.g. in the numerical solution of PDE and integral equations, by Q8 finite element method.

*Acknowledgements*

We thank the authors of [7] for providing the code of their GR cubature, in order to compare their results with ours.

The first author also thanks the National Natural Science Foundation of China (Nos. 60533060, 10726067) and the Natural Science Foundation for Doctoral Career of Liaoning Province of China (No. 20061060) for their support to his research.

## References

[1] P. Bose, G. Tousaint, No quadrangulation is extremely odd, in *Algorithms and Computations*, Lecture Notes in Comput. Sci., Springer Verlag, Berlin 1004 (1995), 372-381.

[2] Richard L. Burden, J. Douglas Faires, *Numerical analysis*, 8th Ed., Thomson Brooks/Cole, Belmont, CA, 2005.

[3] G. Farin, Triangular Bernstein-Bézier patches, Computer Aided Geometric Design, 3 (1986), 83-127.

[4] V. I. Krylov, Approximate Calculation of Integrals, The Macmillan Co., New York London, 1962.

[5] Chong-Jun Li, Ren-Hong Wang, A new 8-node quadrilateral spline finite element, J. Comp. Appl. Math., 195 (2006) 54-65.

[6] A. Ralston, P. Rabinowitz, *A first course in Numerical Analysis*, 2nd Ed., Dover, Mineola, 2001.

[7] A. Sommariva, M. Vianello, Product gauss cubature over polygons based on Green's integration formula, BIT Numerical Mathematics (2007) 47: 441-453.

[8] A. H. Stroud, Approximate calculation of multiple integrals, Prentice-Hall Series in Automatic Computation, Prentice-Hall, Inc., Englewood Cliffs, N. J., 1971.

[9] Ren-Hong Wang, The structural characterization and interpolation for multivariate splines, Acta Math. Sinica 18 (1975) 91-106.

[10] Ren-Hong Wang, *Multivariate Spline Functions and Their Applications*, Science Press/ Kluwer Academic Publishers, Beijing/ New York/ Dordrecht/ Boston/ London, 2001.

[11] O. C. Zienkiewicz, R. L. Taylor, *The finite element method*, 5th Ed., Elsevier (Singapore) Pte Itd., 2005.

[12] MapleSoft, Maple 8.00, Waterloo Maple Inc., 2002 www.maplesoft.com/

[13] The MathWorks, Matlab, The Language of Technical Computing, Version 7.5, 2007 www.mathworks.com/

[14] Wolfram Research, Mathematica, Version 5.1, 2004 www.wolfram.com/